HHS Public Access

Author manuscript

J Cell Biochem. Author manuscript; available in PMC 2016 May 02.

Published in final edited form as:

J Cell Biochem. 2015 October ; 116(10): 2239–2246. doi:10.1002/jcb.25174.

The Function of Twisted Gastrulation in Regulating Osteoclast Differentiation is Dependent on BMP Binding

Raphael Huntley[1], **Julia Davydova**[2], **Anna Petryk**[3,4], **Charles J. Billington Jr**[5], **Eric D. Jensen**[1], **Kim C. Mansky**[6], and **Rajaram Gopalakrishnan**[1]

[1]Department of Diagnostic and Biological Sciences, University of Minnesota, Minneapolis, MN 55455

[2]Department of Surgery, University of Minnesota, Minneapolis, MN 55455

[3]Department of Pediatrics, University of Minnesota, Minneapolis, MN 55455

[4]Department of Genetics, Cell Biology and Development, University of Minnesota, MN 55455

[5]Department of Pediatrics, Children's National Medical Center, Washington DC 20010

[6]Department of Developmental and Surgical Science, University of Minnesota, MN 55455

Abstract

Proper regulation of osteoclast (OCL) function is critical for normal bone homeostasis. Bone morphogenetic protein (BMP) signaling and its regulation have been shown to have direct effects on OCL differentiation and activity. One of the major modulators of BMP signaling in the extracellular space is the secreted protein twisted gastrulation (TWSG1), which can inhibit BMP signaling and OCL differentiation. In this study we examine specific N-terminal regions of TWSG1 protein that have been previously proposed as BMP binding sites to determine whether TWSG1 binding to BMPs is required for its inhibitory effects on OCLs. We demonstrate that overexpression of wild type TWSG1 suppresses osteoclastogenesis, while overexpression of mutant TWSG1 proteins (W66A and N80Q/N146Q mutants), which cannot bind BMPs, leads to increased BMP signaling, enhanced osteoclastogenesis, increased resorptive activity and expression of OCL-specific genes. Our results show that BMP binding is required for TWSG1-mediated inhibition of OCL formation and function, and validate the critical functional regions within the TWSG1 protein for these interactions.

Keywords

Osteoclast; Bone Morphogenetic Protein; Twisted Gastrulation

To whom correspondence should be addressed: Rajaram Gopalakrishnan, 16-108A Moos Tower, 515 Delaware St SE, Minneapolis, MN 55455 Tel: (612) 624-0918, Fax (612) 626-3076, gopal007@umn.edu and Kim Mansky, 16-262b Moos Tower, 515 Delaware St SE, Minneapolis, MN 55455, Tel.: (612) 626-5582, FAX: (612) 626-2571, kmansky@umn.edu.

Introduction

The skeleton is a dynamic structure that is under persistent anabolic, catabolic, and metabolic demands. The fragile balance of bone homeostasis requires constant bone remodeling to maintain a structure that is durable, yet from which calcium ions can be quickly drawn. In many diseases such as osteoporosis, bone resorption outpaces bone formation and bone mineral deposition leading to a net loss in bone mineral density and bone structure. The cells that are primarily responsible for bone resorption are osteoclasts (OCLs), specialized cells derived from hematopoietic stem cells of the monocyte/macrophage lineage. OCLs differentiate in a stepwise fashion to first form mononuclear pre-osteoclast cells (pre-OCLs). Pre-OCLs fuse and spread to form mature multinucleated osteoclasts largely under the regulation of two cytokines: receptor activator of nuclear factor kappa-B ligand (RANKL) and macrophage colony-stimulating factor (M-CSF) (Ross. 2006).

Bone morphogenetic proteins (BMPs) have been well studied as stimulators of osteoblast differentiation and bone formation (Kanatani et al. 1995). However, we recently showed that BMPs are also critical for OCL formation as mice deficient in bone morphogenetic receptor II (BMPRII) in OCLs showed reduced ability to form OCLs (Broege et al. 2013). Further, in support of these *in vivo* findings, bone marrow derived cultures treated with recombinant BMP2 showed increased RANKL-mediated osteoclastogenesis (Jensen et al. 2010). These results suggest that BMPs, acting on OCLs, play a larger role than previously perceived in regulating osteoclast differentiation and potentially in the bone remodeling process.

BMP signaling can be modulated through several extracellular and intracellular mechanisms. In the extracellular space, a major regulatory mechanism is through binding of secreted BMP ligands to BMP binding proteins such as Noggin, Chordin and Twisted gastrulation (TWSG1) (Walsh et al. 2010). Our lab has demonstrated that mice deficient for TWSG1 have enhanced osteoclastogenesis without a defect in bone formation, due to increased BMP signaling (Sotillo Rodriguez et al. 2009). Furthermore, TWSG1 overexpression in pre-OCLs reduces TRAP positive multinucleated OCL formation by suppressing BMP signaling (Pham et al. 2011). We propose that the biochemical basis for the skeletal phenotype in *Twsg1*$^{-/-}$ mice is solely due to lack of TWSG1 binding to BMP ligands and enhanced BMP signaling in OCLs (Sotillo Rodriguez et al. 2009).

The goal of the current project was to investigate whether TWSG1 binding to BMPs is required for its inhibitory effects on OCLs. Towards this end, we investigated the significance of two previously proposed BMP binding sites in TWSG1 (two glycosylation sites within exon 4 and a conserved cysteine rich site in the N-terminus) for inhibition of BMP signaling during osteoclastogenesis. Mutations of these sites on TWSG1 protein, referred to as N80Q/N146Q for glycosylation site mutant (Billington et al. 2011) and W66A for the N-terminal cysteine site mutant (Oelgeschlager et al. 2003) have been shown to have decreased BMP ligand binding ability, but were still able to bind to other extracellular cysteine rich proteins (Oelgeschlager et al. 2003,Billington et al. 2011). Biological effects of these mutations were previously studied in the context of craniofacial development in mice and embryonic patterning in amphibians. Our work aims to understand the impact of these

mutations on osteoclast function. These TWSG1 mutant constructs, along with WT-TWSG1, were overexpressed in pre-OCL. As we have previously shown, WT-TWSG1 expression in pre-OCLs decreased formation and activity of mature OCLs. On the other hand, neither the W66A nor the N80Q/N146Q mutants inhibited osteoclastogenesis, indicating that BMP binding is essential for decreasing OCL differentiation. In fact, cells overexpressing either mutant construct showed increased osteoclastogenesis as well as increased BMP signaling, suggesting loss of TWSG1 binding to BMPs may in fact lead to a possible pro-BMP effect, resulting in enhanced osteoclastogenesis. Our results confirm that BMP binding is required for TWSG1-mediated inhibition of OCL formation.

Material and Methods

Mice

Generation and genotyping of *Twsg1*$^{-/-}$ mice was previously described (Petryk et al. 2004). The use and care of the mice in this study was approved by the University of Minnesota Institutional Animal Care and Use Committee.

Harvesting of Bone Marrow and Generation of Osteoclast Cells

Primary bone marrow macrophages were harvested from the femurs and tibiae of 4-week-old WT C57Bl/6 or *Twsg1*$^{-/-}$ mice. The femurs and tibiae were dissected and adherent tissue was removed. The ends of the bones were cut and the marrow was flushed from the inner compartments. The red blood cells (RBC) were lysed from the flushed bone marrow tissue with RBC lysis buffer (150 mM NH4Cl, 10 mM KHCO3, 0.1 mM EDTA, pH7.4) and the remaining cells were plated on 100 mm plates and cultured overnight in OCL media (phenol red-free Alpha-MEM (Gibco) with 5% fetal bovine serum (Hyclone), 25 units/mL penicillin/streptomycin (Invitrogen), 400 mM L-Glutamine (Invitrogen), and supplemented with 1% CMG 14-12 culture supernatant containing M-CSF). The non-adherent cell population, including OCL precursor cells, was then carefully separated, counted and plated at approximately 1.7×10^4 cells/cm^2 in OCL media supplemented with 1% CMG 14-12 culture supernatant. After 48 hours in OCL media supplemented with 1% CMG 14-12 culture supernatant, cells were treated with 1% CMG 14-12 culture supernatant and 30 ng/mL RANKL (R&D Systems) for approximately 5 days, driving differentiation to mature OCLs.

Osteoclast Transduction

Bone marrow macrophages were isolated as described above. Prior to stimulation with RANKL, the cells were incubated with 100 MOI of adenovirus (control, TWSG1, N80Q/N146Q or W66A) for 3h at 37°C in the presence of 1% CMG 14-12 culture supernatant as previously published (Pham et al. 2011). Titering of the adenoviruses was performed using an optical based density measurement (vp/mL). This method was used to determine viral particle density and MOI as previously described in Pham et al. 2011. After 3 hours, media-containing adenovirus was removed and cells were fed with 1% CMG 14-12 culture supernatant and RANKL (30 ng/ml). After five days, RNA was extracted for use in qRT-PCR, protein was extracted for western blotting, or cells were stained for TRAP.

RNA Isolation and Quantitative RT-PCR

Quantitative real-time PCR was performed using the MyiQ Single Color Real-Time PCR Detection System (Biorad). RNA was harvested from cells using Trizol Reagent (Ambion, Life Technologies) and quantified using UV spectroscopy. cDNA was prepared from 1 μg RNA using the iScript cDNA Synthesis Kit (Biorad) as per the manufacturer's protocol. The $2^{\Delta\Delta Ct}$ method was used to analyze expression; in accordance with this method we have previously experimentally determined that our primer sets amplify with similar efficiencies. Experimental genes were normalized to *GAPDH* as indicated in figure legends. *NFATc1* (Forward) 5′ -TCA TCC TGT CCA ACA CCAAA; (Reverse) 5′ -TCA CCC TGG TGT TCT TCC TC; *CTSK* (Forward) 5′-AGG GAA GCA AGC ACT GGA TA; (Reverse) 5′-GCT GGC TGG AAT CAC ATC TT; *DC-STAMP* (Forward) 5′-GGG CAC CAG TAT TTT CCT GA; (Reverse) 5′ -TGG CAG GAT CCA GTA AAA GG.

Immunoblotting

Cell protein lysates were harvested from OCLs in modified RIPA buffer (50mM Tris pH 7.4, 150mM NaCl, 1% IGEPAL, 0.25% sodium deoxycholate, 1mM EDTA) supplemented with Halt Protease & Phosphatase Inhibitor Cocktail (Thermo Scientific). Lysates were cleared by centrifugation at 12,000X*g* at 4°C. Proteins were resolved by SDS-PAGE and transferred to a PVDF membrane (Millipore). Anti-FLAG (DYKDDDDK) antibody was obtained from Cell Signaling. Smad1/5/8 was obtained from Santa Cruz, and phospho-Smad1/5/8 (p-Smad1/5/8) antibody was obtained from Cell Signaling Technology. HRP-conjugated anti-rabbit or anti-mouse were incubated with membranes, washed, and incubated with Amersham ECL Prime Western Blotting Detection Reagent (GE Healthcare). Typically, the membranes were blotted with p-Smad 1/5/8 before being reblotted with total Smad1/5/8 antibody. Blots were stripped with western blot membrane stripping buffer (100 mM glycine, pH 2.5, 200 mM NaCl, 0.1% Tween 20, 0.1% β-mercaptoethanol) for 5 minutes at 50°C. Densitometry analysis was performed on NIH Image J. Individual activation levels were determined by comparing each p-Smad 1/5/8 band to its total Smad 1/5/8 band, and relative expression was determined by comparing individual activation levels to control infected cell culture levels.

TRAP Stain

Primary OCLs were fixed with 4% paraformaldehyde (PFA) and washed with PBS. The cells were then stained for tartrate resistant acid phosphatase (TRAP) expression with tartrate 5 mg, Naphthol AS-MX phosphate, 0.5 mL M, M-Dimethyl formamide, 50 mL acetic acid buffer (1 mL acetic acid, 6.8 g sodium acetate trihydrate, 11.5 g sodium tartrate in 1 L water) and 25 mg Fast Violet LB salt. Cells were then observed and captured with light microscopy and NIH Image J was used to measure and analyze cell area. Cells with three nuclei or more were counted.

Quantitating Nuclei

TRAP stained multinuclear osteoclasts were stained with DAPI to visualize nuclei. Images of cells were captured with light microscopy and total nuclei were quantitated with NIH Image J. To calculate number of nuclei per cell, DAPI images were overlaid with TRAP

stained images to calculate number of nuclei per cell in TRAP positive cells containing 3 or more nuclei.

Resorption Assays

Osteoclast precursors were plated on Osteo Assay Surface plates (Corning) at a concentration of 100,000 cells per well. Cells were allowed to fully differentiate. On day 5, the media was completely removed and 100μL/well of 10% bleach was added to each well and incubated at room temperature for 5 minutes. The bleach solution was then aspirated off and the wells were washed twice with 150μL of dH_2O. The plate was then allowed to air dry completely at room temperature for 3–5 hours. The wells were observed at 10x magnification for the formation of resorption pits and images were captured with light microscopy. Images were measured and analyzed using NIH Image J.

Statistics

All experiments were performed at least three times in either duplicate or triplicate as indicated in figure legends. The data shown are representative of the mean + SD of all experiments. Student's t-test or 1 way ANOVA analysis followed by a Tukey's multiple comparison test were used to compare data; $p<0.05$ indicates significance. Statistical analysis was performed using Prism 5 software for Mac OSX.

Results

Engineering and Expression of TWSG1 constructs in OCLs

TWSG1 is a highly conserved 222 amino acid glycoprotein with a secretory signal and a single BMP binding region. The previously published TWSG1 W66A mutant lacks a critical tryptophan in its BMP binding region, rendering it unable to bind BMPs (Figure 1A) (Oelgeschlager et al. 2003). The N80Q/N146Q mutant has two point mutations in critical *N*-glycosylation sites in the exon 4 that result in loss of BMP binding (Figure 1A) (Billington et al. 2011). In order to assess the function of TWSG1 binding to BMPs on osteoclastogenesis, adenovirus constructs for WT-TWSG1 and TWSG1 mutants were generated as previously described (Pham et al. 2011). TWSG1 expression was regulated by the CMV promoter, and mononuclear pre-OCL cells were treated at 100 MOI after 48 hours of M-CSF stimulation. Protein expression of all the TWSG1 expressing constructs was at similar levels as measured by western blot (Figure 1B).

Loss of TWSG1 binding to BMPs results in larger OCLs

Our lab has previously shown that OCLs null for TWSG1 are larger than OCLs from WT mice (Sotillo Rodriguez et al. 2009). In addition, we have demonstrated that overexpression of TWSG1 in pre-OCLs inhibited OCL differentiation, resulting in smaller OCLs (Pham et al. 2011). To determine if BMP binding is necessary for the ability of TWSG1 to regulate OCL differentiation, we transduced OCLs from WT mice with either a control adenovirus or an adenovirus overexpressing WT-TWSG1 or mutant TWSG1 and stimulated differentiation with M-CSF and RANKL. As we have previously reported, TWSG1 overexpression drastically reduced OCL differentiation by reducing the size and number of multinucleated mature OCLs as compared to control viral vector (Figure 2A). Because of the drastic

phenotypic range observed, cell sizes were quantified in groups of three nuclei or more, or ten nuclei or more. The size of multinucleated cells with three or more nuclei was doubled in cell cultures overexpressing TWSG1-mutant constructs relative to control-virus transduced cultures (mean values of control: 0.0162, N80Q/N146Q: 0.0317; W66A: 0.0293; TWSG1: 0.0075 mm^2, Figure 2B). In OCLs overexpressing TWSG1 there were no cells with 10 nuclei or more (Figure 2C). In contrast, overexpression of either the N80Q/N146Q or W66A mutant did not show this repressive effect. On the contrary, N80Q/N146Q and W66A mutants showed a 1.5 fold increase (N80Q/N146Q: 0.2391± 0.0985; W66A: 0.2211 ± 0.0131 mm^2) in the size of multinucleated TRAP positive OCLs compared to control transduced cultures (control: 0.1528 ± 0.0174 mm^2, Figure 2C).

TWSG1 mutants have increased resorptive activity

We next examined if the enhanced OCL formation observed in cells overexpressing mutant TWSG1 correlated with increased cell activity. We cultured BMMs on calcium phosphate coated plates, transduced with TWSG1 constructs as described above, and then cells were given M-CSF and RANKL to stimulate osteoclast differentiation. Figure 3A shows photomicrographs of synthetic hydroxyapatite mineral surfaces. As we have previously shown, resorption was reduced in TWSG1 expressing cells compared with control adenovirus transduced cultures, although in this case the reduction did not reach statistical significance (Figure 3B, Pham et al. 2011). On the other hand, both mutant constructs led to a multiple fold increase in resorption (N80Q/N146Q: 11.26% area; W66A: 43.78% area), as compared to both control and TWSG1 overexpression (WT-TWSG1: 0.15% area, Figure 3B). Collectively, these data suggest that loss of BMP binding of TWSG1 results in enhanced OCL formation, causing increased bone resorption.

Effect of W66 and N80Q/N146Q on OCLs is mediated through modulation of BMP signaling

TWSG1 has been shown to antagonize BMP signaling in OCLs (Pham et al. 2011). To determine the status of BMP signaling in TWSG1 mutant overexpressing cells, we transduced mononuclear pre-OCLs as previously described (Pham et al. 2011). At day three of OCL differentiation, after 72 hours of RANKL stimulation, cell lysates were collected and western blot analysis was performed to analyze levels of BMP canonical signaling. We have previously shown that BMPs signal through the canonical SMAD pathway in OCLs (Broege et al. 2013, Jensen et al. 2010). In addition to demonstrating that TWSG1 overexpression led to a reduced OCL size, we showed that TWSG1 reduced p-Smad1/5/8 levels (Pham et al. 2011). Here we show that in contrast to control transduced cell cultures, TWSG1 mutant overexpressing OCLs have increased p-Smad1/5/8 levels, suggesting an increase in BMP signaling (Figure 4A, top panel). Densitometry quantification of the bands shows that N80Q/N146Q and W66A mutant cultures have markedly increased p-Smad1/5/8 activation (23.88 and 33.95 times higher, respectively). Blots were then stripped and reprobed to demonstrate that there were no detectable changes in total Smad1/5/8 (Figure 4A, bottom panel). These data suggest that the cellular defects observed with W66A and N80Q/N146Q overexpression are likely caused by a loss of TWSG1 suppressive activity on canonical BMP signaling.

To determine if the source of the BMP in these cultures was from the OCL themselves or from the FBS used in culturing the osteoclasts, C2C12 cells, which are highly responsive to BMP signaling, were cultured in serum free media for three hours then stimulated with the osteoclast culture media (containing FBS) for thirty minutes. Our data show that the OCL culture media stimulated only a slight increase in p-Smad1/5/8 signaling in these cultures, suggesting that the main source of BMP ligands in the OCL cultures comes from the osteoclasts themselves and not the FBS that is used to culture the osteoclasts (Figure 4B).

TWSG1 mutants have increased expression of key OCL genes

To determine how TWSG1 and TWSG1 mutants function to alter OCL-specific gene expression during differentiation, real time RT-PCR was performed with RNA obtained from OCL cultures following transduction with WT-TWSG1 or mutant TWSG1 adenoviral vectors. We observed an inhibition of *NFATc1* (a key OCL specific transcription factor), *DC-STAMP* (a critical OCL fusion gene) and *CTSK* (an important OCL specific marker required for resorption) expression in WT-TWSG1 compared to control transduced cells (TWSG1 *NFATc1:* 5.41, TWSG1 *DC-STAMP:* 1.84, TWSG1 *CTSK:* 155.63; Control *NFATc1:* 9.54, Control *DC-STAMP:* 3.58, Control *CTSK:* 336.62, Figure 5). In agreement with increased OCL formation, cells overexpressing W66A and N80/146Q mutant showed increased OCL gene expression (Figure 5). This increase was most noted in W66A mutant overexpressing cells, with a 3- to 14-fold increase in expression compared to cells transduced with WT-TWSG1 (relative mean expression value for N80/146Q *NFATc1:* 5.93, N80/146Q *DC-STAMP:* 8.45, N80/146Q *CTSK:* 1217.83; W66A *NFATc1:* 16.81, W66A *DC-STAMP:* 16.61, W66A *CTSK:* 2243.69).

TWSG1 mutants do not act in a dominant negative manner

TWSG1 is expressed in OCLs, and protein levels increase throughout differentiation (Pham et al. 2011). This raises the possibility that the W66A and N80Q/N146Q mutants could compete with endogenous TWSG1 and block normal protein function. This mechanism could account for the increased BMP signaling and possibly increased osteoclastogenesis in OCLs overexpressing mutant TWSG1. To determine if the TWSG1 mutants act in a dominant negative manner, control, WT-TWSG1, W66A or N80Q/N146Q adenoviruses were transduced into *Twsg1*$^{-/-}$ pre-OCLs as has been described in previous experiments for WT pre-OCLs, and then cells were stimulated with RANKL and M-CSF to promote OCL differentiation. Cells were fixed and TRAP positive cells containing three nuclei or more were quantitated. As shown in Figure 6, overexpression of W66A and N80Q/N146Q mutants in *Twsg1*$^{-/-}$ derived bone marrow cultures resulted in larger multinucleated OCLs, similar to those in Figure 2. These results indicate that the effects of W66A and N80Q/N146Q TWSG1 mutants do not depend on the presence of an intact endogenous TWSG1 protein, and hence the mutants do not appear to act in a dominant negative manner.

Discussion

BMPs play a large role in stimulating OCL differentiation, fusion, and activity (Jensen et al. 2010), and TWSG1 is able to decrease BMP signaling in OCLs (Pham et al. 2011). In an effort to understand if TWSG1 regulates osteoclastogenesis by BMP binding alone, we

overexpressed wild type TWSG1 and mutant constructs in early mononuclear pre-OCLs. Here we demonstrate that, consistent with our previous findings, WT-TWSG1 overexpression reduced OCL size and function. On the other hand OCLs overexpressing TWSG1 mutants displayed enhanced osteoclastogenesis, increased resorptive activity, and elevated Smad1/5/8 phosphorylation. These data suggest that the suppressive effects of TWSG1 are mediated by binding of the protein to BMPs, because loss of a functional BMP binding domain on TWSG1 promotes osteoclast differentiation, gene expression, and activity.

Previously, we showed that because of loss of its extracellular inhibitor TWSG1, *Twsg1*$^{-/-}$ mice have increase in BMP signaling and enhanced osteoclastogenesis. These mice are osteopenic compared to WT littermates (Sotillo Rodriguez et al. 2009). Therefore, it was of interest to study the effect of TWSG1 on OCLs in isolation to gain further mechanistic insight into TWSG1-mediated regulation of osteoclastogenesis through its interaction with BMP. Previously designed TWSG1 mutants that do not bind to BMP were used in this study along with WT-TWSG1. Our results further establish WT-TWSG1 as a negative regulator of BMP signaling in osteoclasts. In our studies, OCLs overexpressing TWSG1 had reduced osteoclastic gene expression compared to control OCLs. Phenotypically these mature TWSG1 overexpressing OCLs were smaller and had decreased resorption activity, highlighting the impact of TWSG1 on OCL differentiation.

Maintenance of optimal BMP signaling plays a major role in multiple tissue types such as nephrons during development, embryonic mandibular arch, normal postnatal bone homeostasis, and other systems (Billington et al. 2011,Yamada et al. 2014,Petryk et al. 2004,MacKenzie et al. 2009,Zakin and De Robertis. 2004). In murine osteoclasts (as shown here) and mandibular explants (Billington et al. 2011), exogenous TWSG1 acts as a BMP antagonist. In other biological contexts and species, TWSG1 can also have a pro-BMP function depending on its complex interactions with other BMP binding partners. Oelgeschlager et al. demonstrated a pro-BMP effect in *Xenopus* with the xTSG^{W67G} mutant (a homologue of W66A) due to a direct binding between the mutant TWSG1 and Chordin, which stimulated Chordin cleavage by Tolloid zinc metalloproteinase (Oelgeschlager et al. 2003). In that study, TWSG1 formed a trimolecular complex with Chordin and Tolloid, but not BMP. This interaction between TWSG1 and Chordin does not pertain to mature OCLs because they do not express Chordin (Sotillo Rodriguez et al. 2009).

Our results complement previous studies on the role of TWSG1 in regulating BMP signaling in other model systems and also validate the critical functional regions within the TWSG1 protein for these interactions. Oelgeschlager et al. found that xTSG^{W67G}, the homologous mutant to W66A, had a strong ventralizing effect in *Xenopus*, a phenotype commonly associated with overactive BMP signaling (Oelgeschlager et al. 2003). Furthermore, we have previously demonstrated the requirement for *N*-glycosylation of TWSG1 for BMP binding using a mandible explant model (Billington et al. 2011). In agreement with these data, our studies show that the N-glycosylation compound mutant, N80Q/N146Q, could not inhibit BMP canonical signaling, which underscores the importance of glycosylation sites. Although loss of glycosylation and misfolding can lead to protein degradation, the increase in signaling and activity above that of control transduced cells led us to believe that the

W66A and N80Q/N146Q mutants are not being degraded, and still retain a secondary pro-BMP function.

The results presented here suggest a dual function for TWSG1 in OCLs, with the ability to promote or inhibit BMP signaling. WT-TWSG1 serves to inhibit BMP signaling, while N-terminal TWSG1 mutants have increased BMP signaling above that of control transduced cells. These studies support the notion that TWSG1 limits BMP signaling by direct binding to BMPs through its N-terminus. However, we cannot exclude the possibility that TWSG1's conserved C-terminus, which is retained in our mutant constructs, also contributes to the enhancement of BMP signaling, perhaps acting in conjunction with other extracellular proteins that are also involved in BMP gradient maintenance, for example cysteine-rich proteins such as crossveinless-2 (CV2), Noggin, or members of the DAN family of BMP binding proteins. Further research is necessary to elucidate the multiple and complex interactions of TWSG1.

Acknowledgments

This project was supported by NIH R01 AR056642 (R.G.), NIH R01 DE016601 (A.P.) and NIH T90 DE022732 (R.H.).

Literature Cited

Billington CJ Jr, Fiebig JE, Forsman CL, Pham L, Burbach N, Sun M, Jaskoll T, Mansky K, Gopalakrishnan R, O'Connor MB, Mueller TD, Petryk A. Glycosylation of Twisted Gastrulation is Required for BMP Binding and Activity during Craniofacial Development. Front Physiol. 2011; 2:59. [PubMed: 21941513]

Broege A, Pham L, Jensen ED, Emery A, Huang TH, Stemig M, Beppu H, Petryk A, O'Connor M, Mansky K, Gopalakrishnan R. Bone morphogenetic proteins signal via SMAD and mitogen-activated protein (MAP) kinase pathways at distinct times during osteoclastogenesis. J Biol Chem. 2013; 288:37230–37240. [PubMed: 24235143]

Jensen ED, Pham L, Billington CJ Jr, Espe K, Carlson AE, Westendorf JJ, Petryk A, Gopalakrishnan R, Mansky K. Bone morphogenic protein 2 directly enhances differentiation of murine osteoclast precursors. J Cell Biochem. 2010; 109:672–682. [PubMed: 20039313]

Kanatani M, Sugimoto T, Kaji H, Kobayashi T, Nishiyama K, Fukase M, Kumegawa M, Chihara K. Stimulatory effect of bone morphogenetic protein-2 on osteoclast-like cell formation and bone-resorbing activity. J Bone Miner Res. 1995; 10:1681–1690. [PubMed: 8592944]

MacKenzie B, Wolff R, Lowe N, Billington CJ Jr, Peterson A, Schmidt B, Graf D, Mina M, Gopalakrishnan R, Petryk A. Twisted gastrulation limits apoptosis in the distal region of the mandibular arch in mice. Dev Biol. 2009; 328:13–23. [PubMed: 19389368]

Oelgeschlager M, Reversade B, Larrain J, Little S, Mullins MC, De Robertis EM. The pro-BMP activity of Twisted gastrulation is independent of BMP binding. Development. 2003; 130:4047–4056. [PubMed: 12874126]

Petryk A, Anderson RM, Jarcho MP, Leaf I, Carlson CS, Klingensmith J, Shawlot W, O'Connor MB. The mammalian twisted gastrulation gene functions in foregut and craniofacial development. Dev Biol. 2004; 267:374–386. [PubMed: 15013800]

Pham L, Beyer K, Jensen ED, Rodriguez JS, Davydova J, Yamamoto M, Petryk A, Gopalakrishnan R, Mansky KC. Bone morphogenetic protein 2 signaling in osteoclasts is negatively regulated by the BMP antagonist, twisted gastrulation. J Cell Biochem. 2011; 112:793–803. [PubMed: 21328453]

Ross FP. M-CSF, c-Fms, and signaling in osteoclasts and their precursors. Ann N Y Acad Sci. 2006; 1068:110–116. [PubMed: 16831911]

Sotillo Rodriguez JE, Mansky KC, Jensen ED, Carlson AE, Schwarz T, Pham L, MacKenzie B, Prasad H, Rohrer MD, Petryk A, Gopalakrishnan R. Enhanced osteoclastogenesis causes osteopenia in

twisted gastrulation-deficient mice through increased BMP signaling. J Bone Miner Res. 2009; 24:1917–1926. [PubMed: 19419314]

Walsh DW, Godson C, Brazil DP, Martin F. Extracellular BMP-antagonist regulation in development and disease: tied up in knots. Trends Cell Biol. 2010; 20:244–256. [PubMed: 20188563]

Yamada S, Nakamura J, Asada M, Takase M, Matsusaka T, Iguchi T, Yamada R, Tanaka M, Higashi AY, Okuda T, Asada N, Fukatsu A, Kawachi H, Graf D, Muso E, Kita T, Kimura T, Pastan I, Economides AN, Yanagita M. Twisted gastrulation, a BMP antagonist, exacerbates podocyte injury. PLoS One. 2014; 9:e89135. [PubMed: 24586548]

Zakin L, De Robertis EM. Inactivation of mouse Twisted gastrulation reveals its role in promoting Bmp4 activity during forebrain development. Development. 2004; 131:413–424. [PubMed: 14681194]

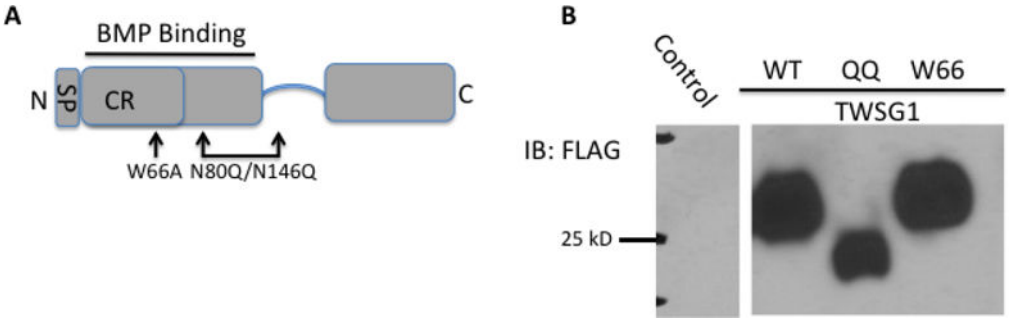

Figure 1. Diagram of TWSG1 protein and expression of TWSG1 mutants

(A) Schematic of TWSG1 showing location of a single BMP binding domain, a secretory signal peptide (SP), and cysteine rich region (CR). Location of point mutations, N80Q/N146Q and W66A, are indicated. (B) Western blot against FLAG epitope of control, wild type (WT), and mutant (QQ and W66) TWSG1 adenoviruses in 293T cells.

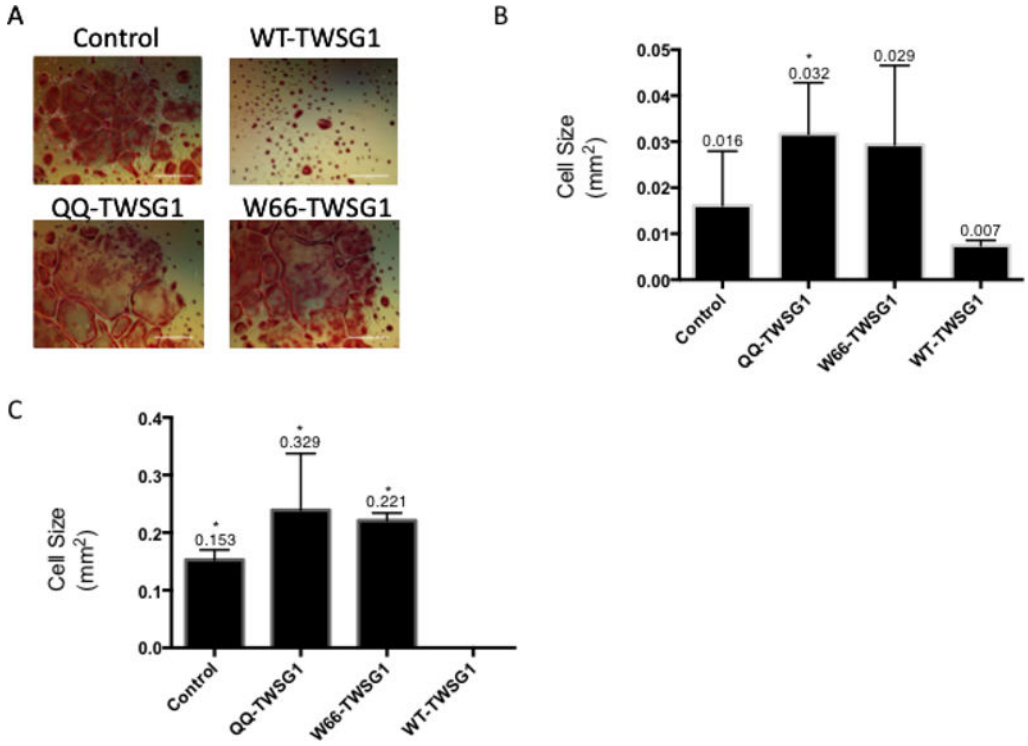

Figure 2. Expression of TWSG1 mutants enhances osteoclast differentiation and size

(A) Images of TRAP positive mature OCLs. Cell area quantification of either control, WT-TWSG1 or mutant TWSG1 adenovirus for cells with three or more nuclei (B) or ten or more nuclei (C). Values represent average of at least three experiments run in triplicate. * indicates statistically significant, with a p value <0.05, compared to WT-TWSG1 transduced cells. Error bars represent standard deviation. Scale bar represents 0.25mm in length.

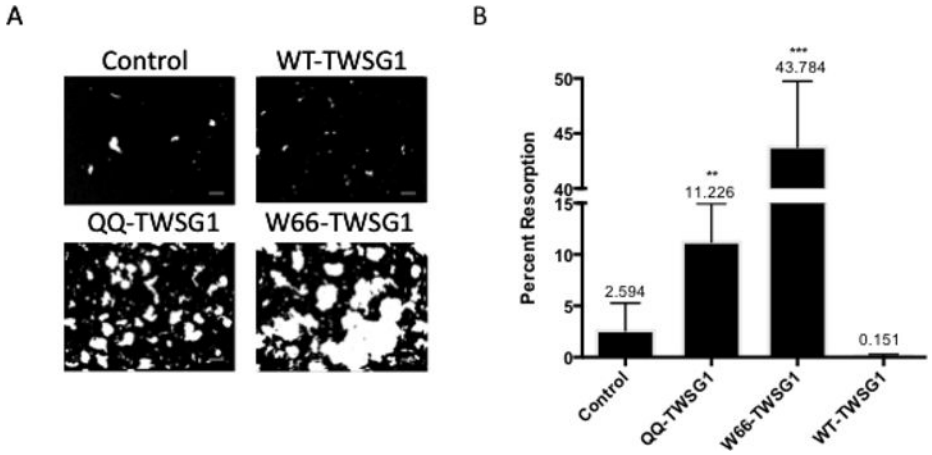

Figure 3. TWSG1 mutant expression increases osteoclast resorptive activity

(A) Binary image of calcium phosphate coated wells. (B) Quantification of percent area resorbed transduced with control, WT-TWSG1 or mutant TWSG1 adenoviruses. Values reflect average of at least three experiments run in duplicate. ** indicates statistically significant compared with a p value <0.005, *** indicates a p value <0.0005, compared to WT-TWSG1 transduced cells. Error bars represent standard deviation. Scale bar represents 0.25mm in length.

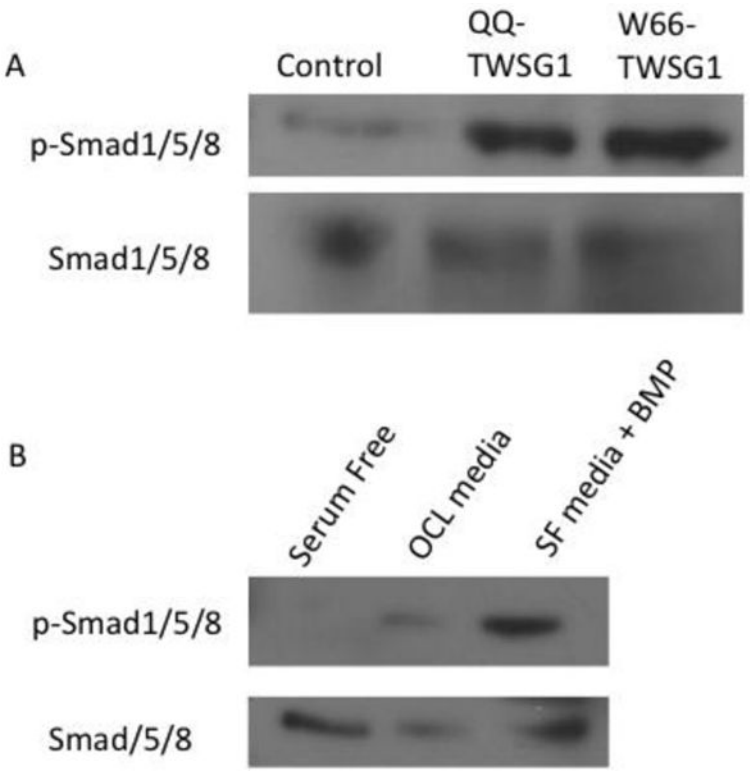

Figure 4. Increased p-Smad1/5/8 activation in osteoclasts expressing TWSG1 mutants

(A) Western blot of osteoclast transduced with control or mutant TWSG1 adenoviruses constructs. Cells were treated with M-CSF and RANKL for 3 days. Cell lysate was analyzed for the presence of p-Smad1/5/8 (Cell Signaling). Blots were striped and reblotted for Smad1/5/8 (Santa Cruz). (B) C2C12 cells starved for three hours then treated with serum free media, OCL differentiation media, or serum free media with 50 ng BMP2. Western blot of cell lysates analyzed for the expression of p-Smad1/5/8 (Cell Signaling), Smad1/5/8 (Santa Cruz).

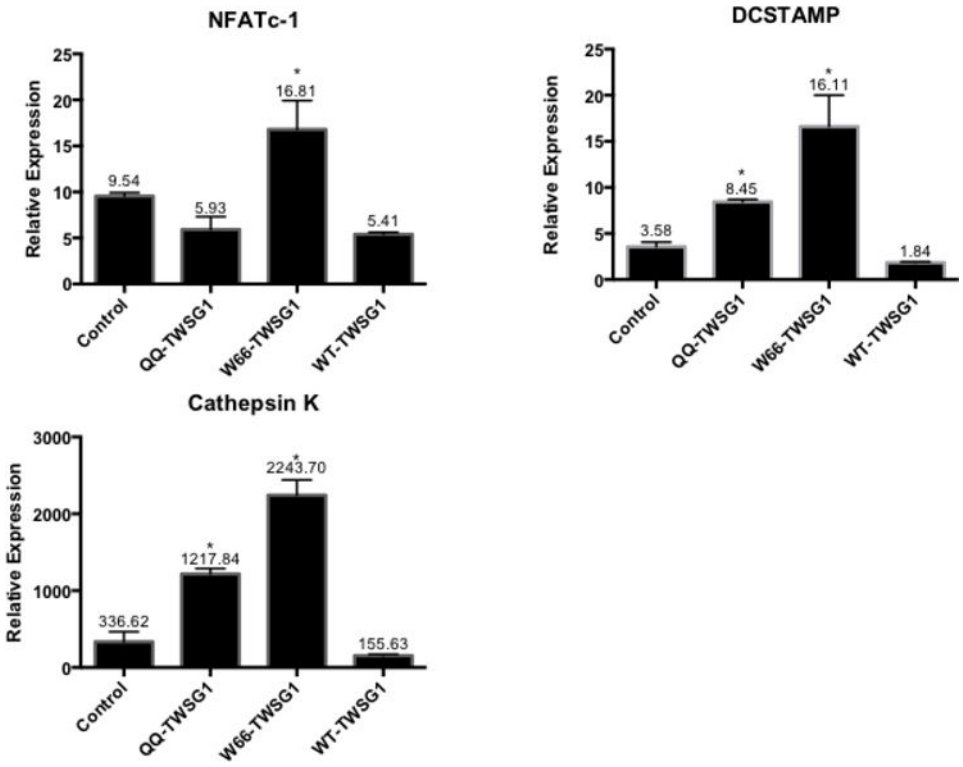

Figure 5. TWSG1 mutant expression increases osteoclast specific gene expression

Real time RT-PCR comparing osteoclast gene expression of *Nfatc1, Dc-stamp* and *cathepsin K* (*Ctsk*) in OCL cultures transduced with control, WT-TWSG1 or mutant TWSG1 adenoviruses. Values were normalized to GAPDH. Values represent the average of at least three experiments run in duplicate. * indicates statistically significant, with a p value <0.05, compared to WT-TWSG1 transduced cells. A one-way ANOVA was used to determine significance. Error bars represent standard deviation.

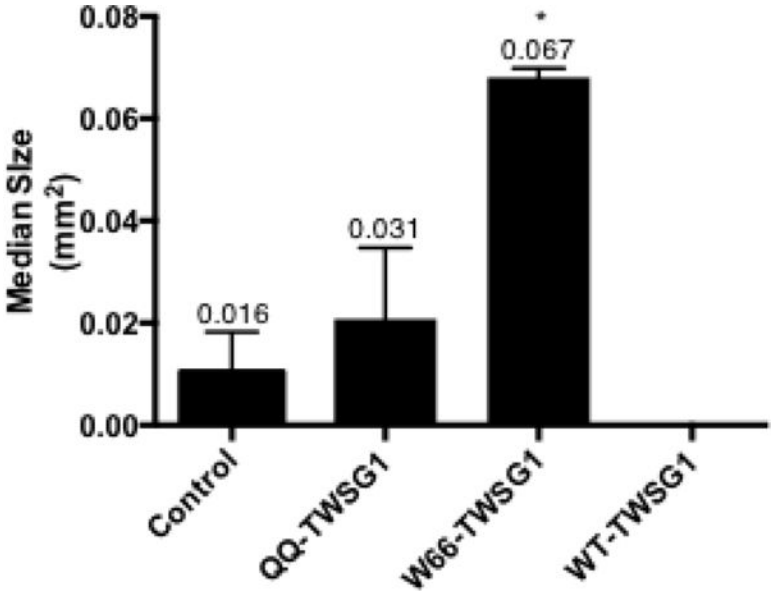

Figure 6. WT-TWSG1 and mutant construct overexpression in *Twsg1*$^{-/-}$ OCL

Quantification of osteoclasts from *Twsg1*$^{-/-}$ mice transduced with control, WT-TWSG1 or mutant TWSG1 adenoviruses. Values represent average of at least three experiments run in duplicate. * indicates statistically significant, with a p value <0.05, compared to WT-TWSG1 transduced cells. Error bars represent standard deviation.